Osteoporos Int (2009) 20:1929–1938
DOI 10.1007/s00198-009-0908-z

ORIGINAL ARTICLE

Radiographic trabecular 2D and 3D parameters of proximal femoral bone cores correlate with each other and with yield stress

D. Steines · S.-W. Liew · C. Arnaud · R. Vargas-Voracek · A. Nazarian · R. Müller · B. Snyder · P. Hess · P. Lang

Received: 18 August 2008 / Accepted: 9 February 2009 / Published online: 25 March 2009

Abstract
Summary Radiographic images of bone cores taken from cadaver proximal femora provided two-dimensional parameters of projected trabecular patterns that correlated highly with conceptually equivalent three-dimensional parameters in the same cores. Measurements also highly correlated with yield stress, suggesting that both parameters have similar biomechanical qualities.
Introduction We compared morphometric measurements of trabecular patterns in two-dimensional (2D) projection radiographic images of cores from cadaver proximal femoral bones with conceptually equivalent measurements from three-dimensional microcomputed tomography (3D μCT) images.
Methods Seven cadaver proximal femora provided 47 excised cores from seven regions. Digitized radiographs of those cores were processed with software that extracts trabecular patterns. Measurements of their distribution, geometry, and connectivity were compared with 3D parameters of similar definition derived from μCT of those cores. The relationship between 2D and 3D measurements and yield stress was also examined.
Results 2D measurements strongly correlated with conceptually equivalent measurements obtained using 3D μCT. In all cases, the correlation coefficients were high, ranging from $r=0.84$ ($p<0.001$) to $r=0.93$ ($p<0.001$). The correlation coefficients between 2D and 3D measurements and yield stress of the cores were also high ($r=0.60$ and 0.82, $p<0.001$, respectively).
Conclusions These findings provide correlative and biomechanical evidence supporting the qualitative similarity of 2D microstructural parameters extracted from

Phase 1 NIH SBIR 1 R43 AR049655

D. Steines · S.-W. Liew · C. Arnaud (✉) · R. Vargas-Voracek · P. Hess
Imaging Therapeutics Inc., 400 Seaport Court, Suite 250,
Redwood City, CA 94063, USA
e-mail: CDA@imatx.com

D. Steines
e-mail: daniel.steines@imatx.com

S.-W. Liew
e-mail: siau-way.liew@imatx.com

R. Vargas-Voracek
e-mail: rene.vargasvoracek@imatx.com

P. Hess
e-mail: Patrick.Hess@imatx.com

A. Nazarian · B. Snyder
Orthopedic Biomechanics Laboratory,
Beth Israel Deaconess Medical Center, Harvard Medical School,
Boston, MA, USA

A. Nazarian
e-mail: anazaria@bidmc.harvard.edu

B. Snyder
e-mail: brian.snyder@childrens.harvard.edu

R. Müller
Institute for Biomechanics, ETH Zurich,
Zurich, Switzerland
e-mail: ram@ethz.ch

P. Lang
ConforMIS Inc.,
Burlington, MA, USA
e-mail: philipp.lang@conformis.com

plain proximal femoral core X-ray images to conceptually equivalent 3D microstructural measurements of those same cores.

Keywords Femur · Microarchitecture · Micro-CT · Radiograph · Yield stress

Introduction

Osteoporosis (OP) is a major public health threat in the United States in terms of mortality, personal debilitation, and health care costs [1]. The most serious consequence of OP is hip fracture. In 2005, the cost of treating hip fractures consumed 72% ($12 billion) of the United States national direct expenditures for OP [1]. By 2025, this is expected to more than double due to an aging population and increasing longevity [2].

The current standard for assessing bone health and strength is to estimate areal bone mineral density (BMD) using dual X-ray absorptiometry (DXA). Recently, it has been also possible to assess proximal femur geometric parameters using DXA-based site-specific measurements of cortical width, but that technology has, so far, failed to capture microstructural features of bone that are also believed to make major contributions to bone strength [3].

Meanwhile, the general use of various iterations of three-dimensional computed tomography (3D μCT) capable of quantifying and imaging bone microstructure in the proximal femur in humans in vivo has not been possible because of excessive radiation exposure attached to that technology. Recognizing the need for alternative solutions, a handful of workers [4–20] have investigated the feasibility of conventional projection radiography (2D) to provide a platform for the measurement of bone microstructure. The earliest studies used microdensitometer-analog computer methods and Fourier transformation techniques [4, 5]. Geraets et al. [6] applied more conventional computer image processing methods and simple geometric measurements on digitized conventional hip radiographs and found differences between subjects without fracture vs. subjects with hip fracture. Ouyang et al. [7] found that texture parameters measured from the radiographic images of excised bone samples correlated significantly with their corresponding BMD measurements and Young's modulus estimated from biomechanical testing. Several groups developed various techniques to assess 2D fractal dimension [8–11] as a global parameter for assessing the complexity of bone structure and its usefulness for characterizing bone quality or strength.

Those studies elicited growing interest in determining how measurements made from 2D projections are related to the dimension and architecture of source structures in 3D. Apostol et al. [12] measured a large number of 2D texture parameters on simulated projection X-ray data derived from 3D μCT data and determined correlations with the 3D parameters. Chappard et al. [13] compared basic bone structural parameters acquired from 2D radiographs of bone blocks in vitro with histomorphometric measurements of those blocks, whereas Jennane et al. [9] validated a mathematical model relating 3D architecture to 2D projection features using 3D μCT images of femoral bone cores and their simulated projections. Some of these methods were based on statistical assessment of texture using fractal techniques [8, 10] rather than direct measurements of structural morphology from 2D images. Pothuaud et al. [14] used 3D magnetic resonance imaging and simulated 2D projection images to compare 2D fractal dimension with 3D trabecular structure. They found significant relationships between 2D fractal dimension and simulated changes in 3D porosity and connectivity, suggesting that changes in fractal dimension can reflect changes in trabecular structure. Similarly, Jennane et al. established and verified a mathematical relationship between 2D and 3D fractal analysis using 3D μCT and simulated projections [9]. Other 2D bone structure parameters that have been studied include texture features based on mathematical morphology [15], measurements of anisotropy [16], and a variety of standard image texture analysis methods [12].

While most of these studies demonstrate the relationship between different microstructural measurements performed on 2D projections with corresponding 3D parameters, the majority used simulated projections of the 3D data and none addressed the important issue of whether the same relationships are maintained with actual 2D projection radiographs, which would be the primary source of direct 2D microstructural measurements in any clinical environment. Simulations of X-rays are limited in value since some magnification and scattering effects are difficult to simulate and can significantly affect image properties. Furthermore, fractal dimension techniques [8, 10] and texture measurements [12, 15] summarize properties such as complexity or visual roughness but do not intuitively relate to the actual morphological and mechanical properties of the corresponding 3D structures. Finally, most studies have either focused on relationships between 2D and 3D measurements or biomechanical properties of bone but have not integrated all three using the same data set.

The present study tests the hypothesis that plain projection radiographs of proximal femoral bone cores are qualitatively sufficient to estimate microstructural (trabecular) core measurements based on their high correlation with 3D μCT measurements of conceptually equivalent parameters in the same cores and their mutual ability to correlate highly with the yield stress of those cores. We approached this by assessing trabecular structure from film-

based radiographic images of bone cores excised from several regions of proximal cadaver femora [17, 18]. Direct morphological measurements from the extracted 2D structures, such as length, thickness, surface area, and perimeter, were made for comparison with equivalent measurements derived from the actual 3D structure. This feature extraction method had several advantages. The 2D measurements obtained, such as dimensions, orientation, spatial distribution, and structural density, are visually verifiable to the extracted structures. They are also more intuitive for linking to conceptually equivalent 3D measurements. Lastly, we directly compared 2D and 3D measurements with their corresponding correlations to yield stress values to determine if our microstructural measurements had biomechanical relevance.

Materials and methods

The data and measurements reported in this study were generated from a sample of bone cores that were previously described [17–19]. In those studies, a total of 47 cylindrical bone cores were obtained from seven deep frozen femora from cadavers of four men (mean 60±9 years old) with no known skeletal pathology. Each femur yielded seven cores (of the total of 49 cores, two cores were not usable and thus excluded). Two cores were extracted from the femoral heads, three from the femoral necks, one from intertrochanteric region and one greater trochanteric region (Fig. 1). The procurement sites were chosen as such to provide representative samples from the major anatomic regions of the proximal femora.

Microcomputed tomography (μCT; μCT20, Scanco Medical, Bassersdorf, Switzerland) was used to image the trabecular architecture in the cored specimens at an isotropic voxel size of 34 μm. The cored specimens were also imaged with high-contrast, high-resolution film projection radiography (Faxitron X-ray Systems, McMinnville, OR, USA) for 27 s at 80 kV setting. The mineral content of the specimens was assessed by DXA measurements (PIXImus2, GE Lunar, Madison, WI, USA). The total mineral content (BMC, in grams) and areal BMD (in grams per square centimeter) were analyzed by drawing a region of interest enveloping the entire specimen. We then obtained the 2D and 3D structural parameters from the radiographs and CT images as described in the sections that follow.

Three-dimensional measurements

For each core, CT volumetric images (512×512 per slice) covering the entire length of the core were reconstructed using standard convolution back projection. The resulting

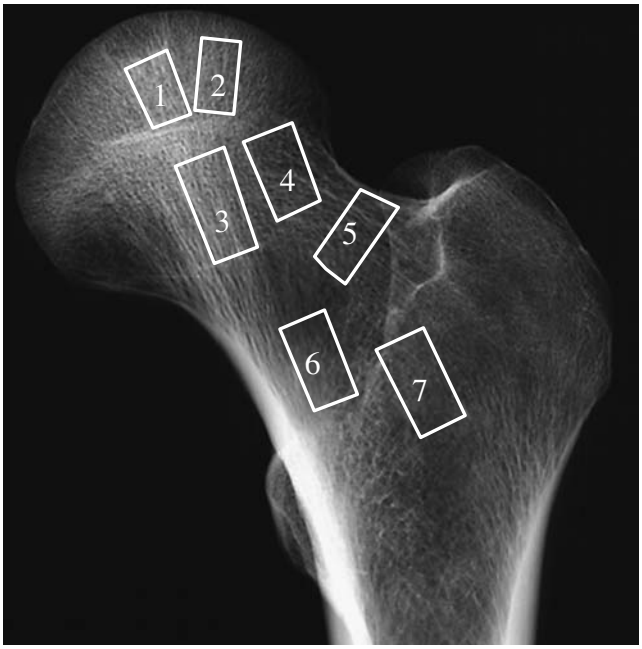

Fig. 1 Regions of bone cores harvested from proximal femoral cadaveric specimen. Bone cores were obtained from seven regions: the medial proximal femoral epiphysis (region *1*), lateral femoral epiphysis (region *2*), the superior medial femoral neck (region *3*), the superior lateral femoral neck (region *4*), the inferior lateral femoral neck (region *5*), inferior medial femoral neck (region *6*), and the trochanteric region (region *7*)

grayscale images were first filtered using a constrained 3D Gaussian filter (width=1.2, support=1) to remove noise and then thresholded to extract the structure of mineralized tissue. Morphometric variables were computed from the binary volume images using direct, 3D measurement techniques with no prior assumptions about the underlying structure [20]. On trabecular structures, we assessed: (1) bone volume fraction (BV/TV, the ratio of 3D total bone volume to the total core volume); (2) bone surface area to total core volume ratio (BS/TV, per millimeter); (3) bone surface area to total bone volume (BS/BV, per millimeter); (4) average trabecular thickness (Tb.Th, in micrometers); (5) trabecular number (Tb.N, the inverse of the mean distance between the mid-axes of the structures, per millimeter); and (6) trabecular separation (Tb.Sp, the mean distance of the nonbone regions, in micrometers). In addition, the nonmetric structural model index (SMI), a measure of trabecular structure shape (plates and rods), was also measured using the methods described in Hildebrand et al. [20].

Two-dimensional measurements

Radiographs of all cores were digitized using a professional desktop scanner (Umax PowerLook 1100) in transparency mode at 1,200 dots per inch or pixel size of 21 μ. Each

digitized radiograph was cropped to a manually delineated, rectangular region of interest that outlined the entire projected bone core image for further automated processing using the software developed by Imaging Therapeutics, Inc. Specifically, the following steps were implemented for the processing of the cropped images of the bone cores.

(1) Each core image was filtered to remove extreme low- and high-frequency background information employing a difference-of-Gaussians (DOG) filter with parameters $sigma_1=10$, $sigma_2=19$ and using kernels with sizes of 15×15 and 29×29, respectively. The resulting images emphasized the structure within a band of special frequencies defined by the parameters of the DOG filter. The parameters of the DOG filter were fine-tuned through an ad hoc iterative procedure starting from an initial parameter selection based on the resolution of the digitization and average dimension of the cores. After background removal, the images were binarized by the gray level values with a threshold value of 0 [6, 21] The resulting binary patterns were then processed through a morphology-thinning-based medial axis transform (*skeletonization*) algorithm to generate the centerlines of the patterns or skeletons [22] (Fig. 2).

(2) The extracted binary patterns, along with their corresponding skeletons, were analyzed to obtain measurements of dimension, such as length, thickness, area, and perimeter. Structure thickness and spacing were estimated by averaging the values of distance

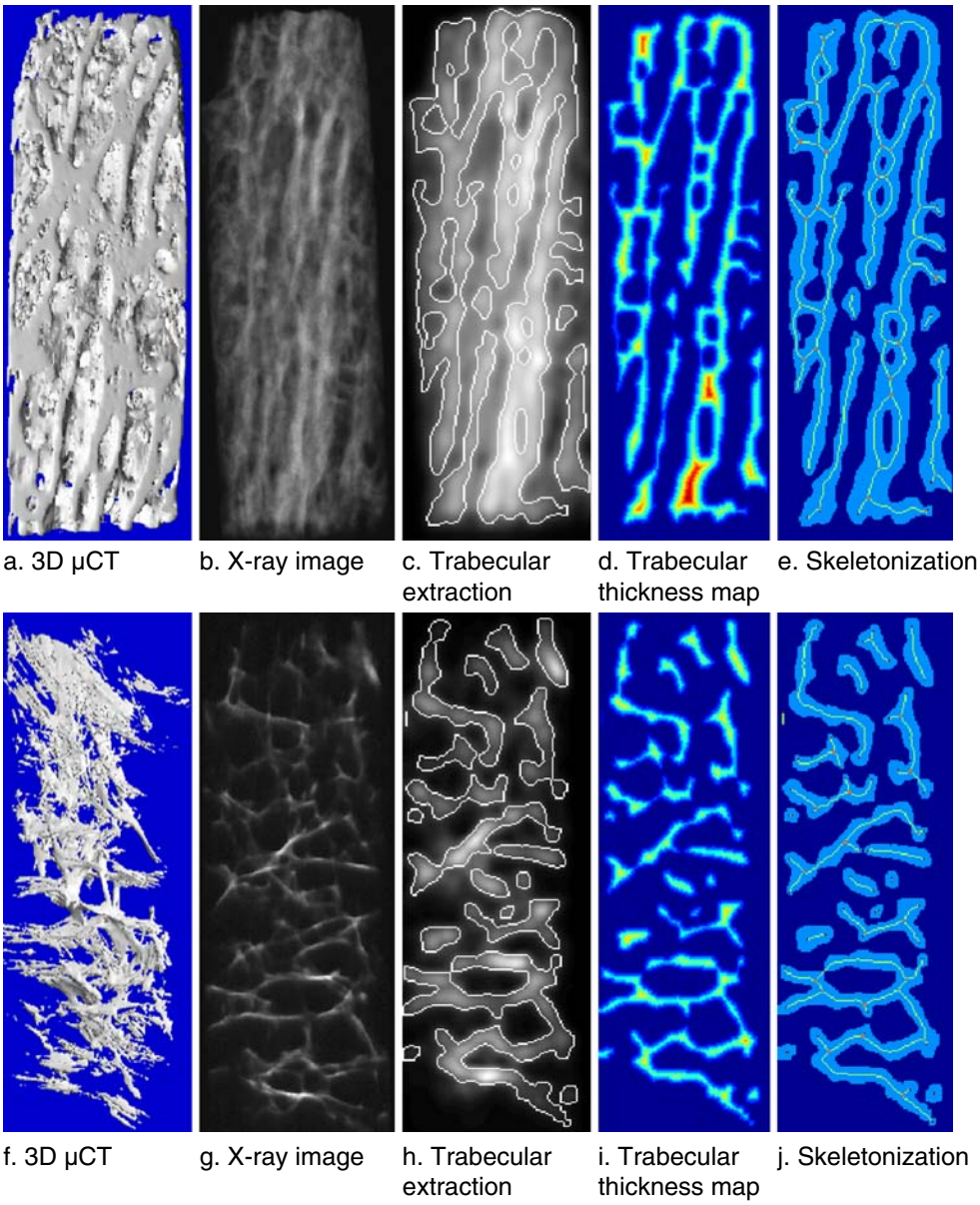

Fig. 2 **a** Representative 3D reconstruction of µCT data obtained from region 3. Of note, the bone harvested from this location is very dense with highly perceivable connectivity. **f** 3D reconstruction of µCT data obtained from region 5. The trabecular microstructure and orientation is substantially different from that of region 3 (in **a**). The X-ray image and 3D reconstruction show visible similarities (**a**, **b**). The X-ray image of the bone core harvested from region 5 also shows perceptible similarities to 3D µCT (**f**, **g**). The remaining images illustrate the processing steps performed on the 2D X-ray data for trabecular microstructure analysis of the two core samples from region 3 and region 5, respectively. In a first step, the trabeculae are extracted from the X-ray image (**c**, **h**). Subsequently, a trabecular thickness map is derived (**d**, **i**). A skeletonization (medial axis transform) of the extracted structures calculated (**e**, **j**)

transform of the binarized structure and background region along their centerlines [22]. This approximates the method presented by Hildebrand et al. [20] but performed on 2D images.

The measurements performed for this study were: (1) area of structure per total core area (Tb.Area/Total Area); (2) total structure perimeter per total core area (Tb.Perimeter/Total Area); (3) total structure perimeter per total bone area (Tb. Perimeter/Tb.Area); (4) average 2D structure thickness (Tb. Thickness); (5) a derived trabecular number (2D Tb.Number, estimated as (Tb.Area×Tb.Thickness)/Total Area) [20]; and (6) average trabecular separation (Tb.Separation). These six 2D measurements were conceptually as similar as possible to the corresponding 3D measurements we made using μCT.

For comparison, fractal dimension was also estimated from the slope of the spectral distribution of intensity values within the region of interest of each core radiograph [23].

Mechanical testing

Following all imaging steps, specimens underwent mechanical testing (uniaxial compressive displacement) using a custom-made micromechanical testing device [19]. Maximum compressive strain of 12% was applied to each specimen at a strain rate of 0.01% s^{-1} following a triangular 0–0.3–0% strain for seven cycles at a strain rate of 0.5% s^{-1}. The yield stress was determined at the point where the stress–strain data became nonlinear using 0.2% strain offset.

Data analysis

Regression analysis was performed on each 2D measurement against the values of its conceptually similar 3D measurement in all 47 cores and with their yield stress. The mean, median, and standard deviation were calculated for radiograph-derived 2D parameters and image-derived 3D parameters. Each 2D parameter was tested individually for its power to correlate with yield stress of the bone cores. Those X-ray-derived trabecular micromeasurements were further tested to determine if they correlated with similar 3D μCT measurements. Correlation coefficients between 2D and 3D measurements were calculated based on robust regression. The correlations within the 2D and 3D groups were also estimated separately. Moreover, we assessed the differences in confidence intervals of correlation coefficients between 2D measurements and yield stress and between 3D measurements and yield stress. Using robust multiple-regression modeling, all 2D parameters were used to predict yield stress. It was then compared to a multiple-regression model using all 3D parameters and to using BMD alone. To study the extent to which each structural parameter accounted for BMD in predicting bone core strength, semipartial correlation coefficients with yield stress were obtained by correlating yield stress with the residuals from linear regressions of BMD to each 2D parameter [24]. Another set of semipartial correlation coefficients was obtained by correlating yield stress with the residuals from regressions of each 2D parameter to BMD, thus illustrating the residual power of each structural parameter after removing BMD dependency. Measurements were also compared by the region of the femur from which the cores where extracted using pairwise comparisons along with a Bonferroni correction of the significance level (p= 0.05/6=0.0083). For each core region, the mean values with corresponding 95% confidence intervals were also calculated. The relationships between 2D and 3D measurements were evaluated for normality and linearity using the Shapiro–Wilk test and standard plots of residuals from robust regression. For nonlinear relationships, the data was transformed logarithmically to approximate the linearity assumptions.

Results

Table 1 presents the Pearson's correlation coefficients between projection radiograph 2D proximal femoral core measurements and corresponding 3D measurements from

Table 1 Correlation coefficients of measurements with yield stress and between conceptually equivalent 2D and 3D parameters

2D measurements (X-ray images)	2D yield stress (r)	3D measurements (μCT images)	3D yield stress (r)	2D–3D correlation (r)
Tb.Area/Total Area	0.73	BV/TV	0.79	0.90
Tb.Perimeter/Total Area	0.60	BS/TV	0.66	0.91
Tb.Perimeter/Tb.Area	−0.77	BS/BV	−0.79	0.93
2D Tb.N	0.67	Tb.N	0.67	0.93
Tb.Thickness	0.81	Tb.Th	0.82	0.84
Tb.Separation	−0.62	Tb.Sp	−0.64	0.88
Fractal dimension	−0.35	SMI	−0.76	0.49

μCT images Each 2D measurement shown was paired with a corresponding 3D measurement based on their close conceptual association, not based on the degree of correlation. Thus, the paired comparisons were between:

(1) Bone volume fraction (BV/TV) and 2D Tb.Area/Total Area;
(2) 3D BS/TV and 2D Tb.Perimeter/Total Area;
(3) 3D BS/BV and 2D Tb.Perimeter/Tb.Area;
(4) 3D Tb.N and 2D Tb.Number;
(5) 3D Tb.Th and 2D Tb.Thickness; and
(6) 3D Tb.Sp. and 2D Tb.Separation.

For reference and comparison, the correlations between 2D-derived fractal dimension and 3D measurements, as well as correlations between the 3D SMI and 2D measurements were also calculated. The correlation coefficients between similar 2D and 3D parameters in Table 1 ranged from r=0.84 to r=0.93 (example illustrated in Fig. 3a). Table 1 also demonstrates the corresponding correlation coefficients of 2D and 3D measurements with yield stress across both modalities (example plots of 2D and 3D parameters correlations are illustrated in Fig. 3b, c, respectively). Moreover, when patterns of cross-correlations within a modality are compared across modalities (Tables 2 and 3), they show similar trends, i.e., being positive, negative, higher, or lower.

When mean values of 2D measurements from cores of the seven sites (Fig. 1) were compared, no significant difference could be identified, whereas there was a difference between the mean 3D parameter values from site 2 (femoral head) and the sites in the trochanteric region (5 through 7) as previously reported [19]. However, when the mean values of 2D measurements were grouped by core region (1 through 4 and 5 through 7), a significant difference was demonstrated (p=0.008) in all parameters except for Tb.Thickness and fractal dimension.

Absolute correlation values between 2D measurements and yield stress ranged between 0.35 (for fractal dimension) and 0.81 (for Tb.Thickness). In multiple-regression modeling, the adjusted correlation coefficient was 0.81 between yield stress and all 2D parameters as predictors and 0.82 between yield stress and all 3D parameters. The correlation coefficient between yield stress and BMD alone was r= 0.82 and the addition of 2D or 3D measurements to BMD in multiple-regression analysis did not alter this value.

Semipartial correlations between yield stress and 2D and 3D structural measurements and also with structure and BMD dependency adjustments are shown in Tables 4 and 5. Adjusting for either 2D or 3D parameters resulted in loss of power in three out of seven sets to predict yield stress with BMD (Tb.Area/Total Area and BV/TV; Tb.Perimeter/Tb. Area and BS/BV; and Tb.Thickness and Tb.Th) but retained the power to predict yield stress with the remainder of the parameters. In sharp contrast, BMD adjustment resulted in a total loss in power to predict yield stress for all 2D and 3D parameters.

Discussion

The major findings in this study are that (1) measurements of 2D structures extracted from plain radiographs of human cadaver proximal femoral cores that intuitively appear to be similar to established 3D μCT trabecular parameters correlate highly with actual 3D μCT measurements of those parameters; (2) those 2D and 3D trabecular measurements individually correlate with yield stress of the femoral cores; and (3) the removal of BMD contribution in a semipartial correlation analysis of a two-parameter model

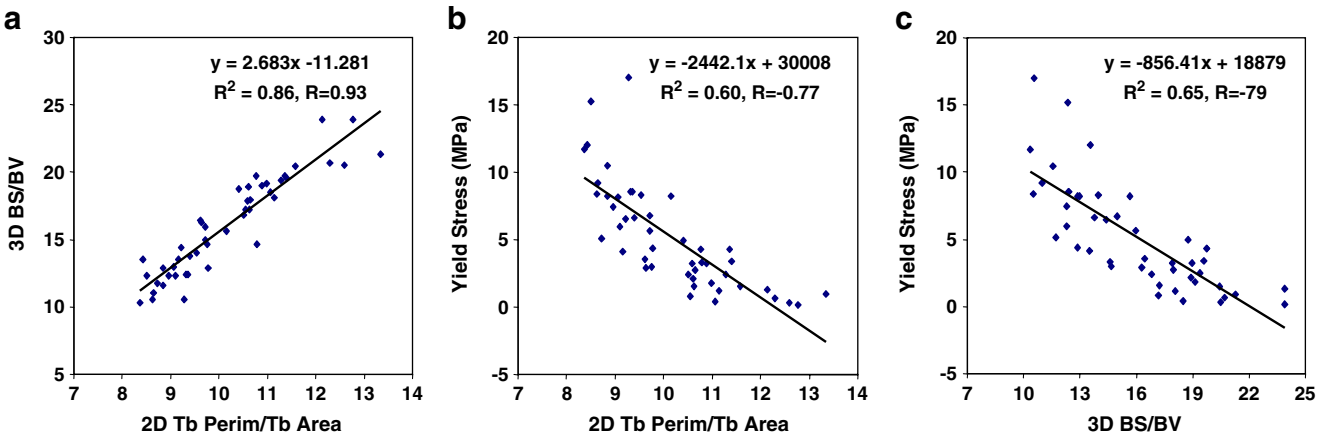

Fig. 3 Graphical illustration of the distribution and correlation between **a** an example 3D parameter (BS/BV) and the corresponding 2D parameter (Tb.Perimeter/Tb.Area), **b** the same 2D parameter and yield stress, **c** the corresponding 3D parameter and yield stress

Table 2 Correlation coefficients within 2D measurement

2D parameters	Tb.Area/ Total Area	Tb.Perimeter/ Total Area	Tb.Perimeter/ Tb.Area	2D Tb.N	Tb.Thickness	Tb.Separation	Fractal dimension
Tb.Area/Total Area	–	0.95	−0.94	0.73	0.84	−0.95	−0.66
Tb.Perimeter/ Total Area	0.95	–	−0.81	0.79	0.69	−0.98	−0.68
Tb.Perimeter/ Tb.Area	−0.94	−0.81	–	−0.59	−0.94	0.82	0.60
2D Tb.N	0.73	0.79	−0.59	–	0.40	−0.78	−0.64
Tb.Thickness	0.84	0.69	−0.94	0.40	–	−0.70	−0.48
Tb.Separation	−0.95	−0.98	0.82	−0.78	−0.70	–	0.65
Fractal dimension	−0.66	−0.68	0.60	−0.64	−0.48	0.65	–

(BMD combined with 2D or 3D measurements) to predict yield stress abolished the significance of the residual correlations, whereas the removal of the contribution of structural parameters only partially reduced the residual correlation of BMD for the corresponding 2D and 3D structural parameters.

The present study uses radiographic images as a source for the measurement of trabecular structural features and, therefore, requires that 2D projected structures are reliably extracted from underlying background and noise. The 2D segmentation of structures also depends on image characteristics such as contrast and resolution. Moreover, the shape of projected structures is dominated by the densest structure in a projected X-ray path and density is affected by overlapping of trabecular structures. The presented techniques take advantage of some of the commonly known algorithms [6, 21, 22] in the field of digital image processing to compensate for variations in radiographic imaging conditions, giving rise to meaningful data that otherwise might have seemed latent.

Since the results of this study are based on the evaluation of bone core specimens, their generalization to the analysis of entire bones ex vivo or in vivo is limited. Further experimentation is necessary to assess the effect of cortical bone, bone marrow, and soft tissue. Finally, it is important to recognize that the 2D parameters do not provide true quantitative measurements of the physical bone structure, but rather a statistical assessment.

The first major finding supports our hypothesis that it is possible to make reasonable estimations of established trabecular parameters from plain, projection radiographs of cadaver proximal femoral bone cores. The correlation coefficients obtained between 2D and 3D measurements are similar to those obtained by Chappard et al. [13] for trabecular bone volume, thickness, separation, and number in human iliac crest biopsies using μCT (3D), unstained biopsy sections (2D), and stained histological sections (H). These correlation coefficients ranged between r=0.69 (3D vs. 2D) and r=0.96 (2D vs. H) for trabecular separation and bone volume, respectively. For comparison, Table 1 shows "r values" of 0.88 and 0.90 (2D vs. 3D) for the same parameters. Moreover, a within modality comparison of coefficients in Tables 2 and 3 of the present study shows similar absolute values and direction of correlations between equivalent parameters across modalities supporting the probable validity of the pairings of parameters by conceptual definition.

The statistically significant regional differences in mean 2D measurements we found when the seven core regions were grouped into two major regions (1–4 and 5–7) further suggests 2D–3D concurrence, albeit with lower sensitivity than the 3D values due to the need for regional grouping. It is possible that

Table 3 Correlation coefficients within 3D measurement

3D parameters	BV/TV	BS/TV	BS/BV	Tb.N	Tb.Th	Tb.Sp	SMI
BV/TV	–	0.91	−0.94	0.91	0.95	−0.85	−0.94
BS/TV	0.91	–	−0.80	0.99	0.76	−0.95	−0.84
BS/BV	−0.94	−0.80	–	−0.80	−0.98	0.79	0.89
Tb.N	0.91	0.99	−0.80	–	0.76	−0.95	−0.84
Tb.Th	0.95	0.76	−0.98	0.76	–	−0.72	−0.91
Tb.Sp	−0.85	−0.95	0.79	−0.95	−0.72	–	0.78
SMI	−0.94	−0.84	0.89	−0.84	−0.91	0.78	–

Table 4 Semipartial correlations with yield stress, adjusting for 2D or BMD

2D parameters	r (BMD, yield stress|2D)[a]	r (2D, yield stress|BMD)[b]
Tb.Area/Total Area	0.329	0.073
Tb.Perimeter/Total Area	0.551*	0.078
Tb.Perimeter/Tb.Area	0.237	−0.106
2D Tb.N	0.763*	−0.228
Tb.Thickness	0.213	0.179
Tb.Separation	0.523*	−0.142
Fractal dimension	0.747*	−0.004

*$p<0.025$, significant correlation estimates

[a] Semipartial correlation between BMD and yield stress adjusted for the effect of a structural parameter

[b] Semipartial correlation between structural parameter and yield stress adjusted for the effect of BMD

this could be caused by compression of 3D structural information when it is projected into a single 2D plane with 3D–2D compression being more pronounced when the density of structures increases as more of them overlap in the 2D plane. This effect would be expected to only blunt the expression of 3D structures as 2D images (as appears to be the case) because the dominant structure within a particular core is also reflected as a dominant feature in the 2D plane, thus reducing the sensitivity of the 2D structural measurements.

The second major finding in this study that the 2D and 3D measurements we made correlate significantly with yield stress of the femoral cores provides evidence that supports a biomechanical role for those trabecular structures. Most importantly, the differences between those 2D and 3D correlation coefficients are not significant, suggesting that 2D measurements approach the ability of μCT to predict the mechanical competence of the cores. These correlations between 2D structural parameters and yield stress are slightly higher than the ones reported for similar bone structural parameters measured from projectional X-rays by Ouyang et al. [7].

The third major finding of the study relates to the experiments we performed that attempted to determine the relative importance of BMD as opposed to structure to the correlation of 2D and 3D measurements with yield stress. In the regression models to predict stress, the correlation coefficient given by the 2D model is not statistically different from that produced by the 3D model and both have nearly identical values as the correlation between BMD and yield stress. Furthermore, multiple-regression analysis of structural parameters from each modality (2D or 3D) failed to improve the correlation of BMD with yield stress. This set of observations led to the question of whether structural parameters provide information independent of BMD in predicting yield stress in bone cores. The semipartial correlation analysis in Tables 4 and 5 shows that the removal of the contribution of BMD in each two-parameter model (BMD combined with 2D or 3D structure) to predict yield stress reduced residual correlation coefficients to nonsignificant levels (right column). A similar effect was observed when three out of seven of the same sets of 2D or 3D structural parameters were removed. We have interpreted these observations to indicate that there is overlap of information provided by BMD and trabecular structure in predicting yield stress, but that BMD predominates. This is to be expected as X-ray imaging of bone depends on mineralization of the tissue. Parfitt made a point of this in 1992 [30], emphasizing that the contribution of bone architecture to bone strength is partly captured by density as both usually vary in the same way. Such overlap is similar to that observed in previous work using vertebral bone cubes [25], calcaneal cores [26], vertebral biopsies [27], whole distal radius [28], and whole proximal femur [29].

All of these studies, as well as ours, conclude that BMD is the major contributor to the strength of trabecular bone, no matter whether it is studied in small isolated cores, cubes, biopsies, or on small regions of interest in whole cadaver bones. It is our opinion that such an explanation is especially valid in samples of fairly small dimensions (such as the ones used in this study) in which material composition can be assumed to be constant. In whole bone, however, where such constancy cannot be guaranteed, it is possible that special techniques are needed to demonstrate the contribution of microstructure to bone strength. This is

Table 5 Semipartial correlations with yield stress, adjusting for 3D or BMD

3D parameters	r (BMD, yield stress|3D)[a]	r (3D, yield stress|BMD)[b]
BV/TV	0.239	−0.154
BS/TV	0.488*	−0.040
BS/BV	0.259	0.054
Tb.N	0.488*	−0.040
Tb.Th	0.230	0.031
Tb.Sp	0.486*	−0.190
SMI	0.368*	−0.067

*$p<0.025$, significant correlation estimates

[a] Semipartial correlation between BMD and yield stress adjusted for the effect of a structural parameter

[b] Semipartial correlation between structural parameter and yield stress adjusted for the effect of BMD

illustrated by a recent publication of Keaveny et al. [31], who report a study of the effects of parathyroid hormone on proximal femoral bone strength in humans. Using finite element analysis, they showed that changes in trabecular bone dominated femoral strength changes (increase), whereas changes in cortical bone and bone geometry made a relatively smaller contribution.

It is likely that, in whole femur, cortical bone properties (density, thickness, composition) together with bone geometry and trabecular properties (architecture, density, composition) are all significant contributors to bone strength. The present study assessed only the trabecular properties independent of their roles in the contribution to whole bone strength. The significance of structural measurements in whole bone, where trabecular architecture may be analyzed in larger areas, still needs to be assessed in the context of their relationships with cortical bone properties and whole bone geometry. But for this purpose, the 2D–3D conceptual link we have established in the present paper could allow rational 2D parameter selection based on the understanding of the mechanical behavior of 3D structural properties. Additionally, the methods detailed in the present study may allow an evaluation of bone structure in vivo that traditional DXA BMD measurement cannot provide, i.e., the assessment of trabecular properties and their contribution to the total BMD and total bone quality. For example, such an approach could prove to be useful in therapy monitoring where different drugs may cause varying degrees of response in cortical bone and trabecular bone. Thus, the fact that structural measurements in this bone core study did not add much additional value to BMD in the assessment of core yield stress does not preclude their potential importance in whole bone strength assessments [18] and the development of a fracture prediction algorithm [32].

In conclusion, this study demonstrates that 2D radiograph-based measurements of trabecular structure in proximal femoral bone cores are related to 3D trabecular structures as assessed by 3D μCT and have mechanical significance. If they are shown to be as valid when applied to whole proximal femur radiographs, they could play an important role in the clinical and experimental assessment of proximal femur bone quality and have the potential to become an effective, widely available, and economically viable alternative method for assessing OP.

Conflicts of interest Dr. Steines, Dr. Arnaud, Mr. Liew, and Dr. Vargas-Voracek are employees of Imaging Therapeutics Inc. and own stock in the company. Dr. Lang and Dr. Hess are members of the board of directors of Imaging Therapeutics Inc. and own stock in the company. All other authors have no conflicts of interest.

References

1. Melton LJ 3rd (2003) Adverse outcomes of osteoporotic fractures in the general population. J Bone Miner Res 18:1139–1141
2. Burge R, Dawson-Hughes B, Solomon DH, Wong JB, King A, Tosteson A (2007) Incidence and economic burden of osteoporosis-related fractures in the United States, 2005–2025. J Bone Miner Res 22:465–475
3. Seeman E, Delmas PD (2006) Bone quality—the material and structural basis of bone strength and fragility. N Engl J Med 354:2250–2261
4. Rockoff SD, Zettner A, Albright J (1967) Radiographic trabecular quantitation of human lumbar vertebrae in situ. II. Relation to bone quantity, strength and mineral content (preliminary results). Invest Radiol 2:339–352
5. Rockoff SD (1967) Quantitative microdensitometric x-ray analysis of vertebral trabecular bone. A preliminary report. Radiology 88:794–796
6. Geraets WGM, van der Stelt PF, Lips P, van Ginkel FC (1998) The radiographic trabecular pattern of hips in patients with hip fractures and in elderly control subjects. Bone 22:165–173
7. Ouyang X, Majumdar S, Link TM, Lu Y, Augat P, Lin J, Newitt D, Genant HK (1998) Morphometric texture analysis of spinal trabecular bone structure assessed using orthogonal radiographic projections. Med Phys 25:2037–2045
8. Caligiuri P, Giger ML, Favus M (1994) Multifractal radiographic analysis of osteoporosis. Med Phys 21:503–508
9. Jennane R, Harba R, Lemineur G, Bretteil S, Estrade A, Benhamou CL (2007) Estimation of the 3D self-similarity parameter of trabecular bone from its 2D projection. Med Image Anal 11:91–98
10. Lin JC, Grampp S, Link T, Kothari M, Newitt DC, Felsenberg D, Majumdar S (1999) Fractal analysis of proximal femur radiographs: correlation with biomechanical properties and bone mineral density. Osteoporos Int 9:516–524
11. Majumdar S, Weinstein RS, Prasad RR (1993) Application of fractal geometry techniques to the study of trabecular bone. Med Phys 20:1611–1619
12. Apostol L, Boudousq V, Basset O, Odet C, Yot S, Tabary J, Dinten JM, Boiler E, Kotzki PO, Peyrin F (2006) Relevance of 2D radiographic texture analysis for the assessment of 3D bone micro-architecture. Med Phys 33:3546–3556
13. Chappard D, Retailleau-Gaborit N, Legrand E, Basle MF, Audran M (2005) Comparison insight bone measurements by histomorphometry and microCT. J Bone Miner Res 20:1177–1184
14. Pothuaud L, Benhamou CL, Porion P, Lespessailles E, Harba R, Levitz P (2000) Fractal dimension of trabecular bone projection texture is related to three-dimensional microarchitecture. J Bone Miner Res 15:691–699
15. Veenland JF, Grashius JL, van der Meer F, Beckers AL, Gelsema ES (1996) Estimation of fractal dimension in radiographs. Med Phys 23:585–594
16. Luo G, Kinney JH, Kaufman JJ, Haupt D, Chiabrera A, Siffert RS (1999) Relationship between plain radiographic patterns and three-dimensional trabecular architecture in the human calcaneus. Osteoporos Int 9:339–345
17. Arnaud CD, Liew S, Steines D, Nazarian A, Mueller R, Linder BJ, Lang P (2003) Correlation of 2D trabecular structure parameters with 3D μCT and measurements of bone strength in femoral bone cores. J Bone Miner Res 18(Suppl 2):S56
18. Arnaud CD, Steines D, Liew S, Nazarian A, Snyder B, Linder BJ, Lang P (2003) Fracture load of fresh-frozen cadaveric proximal femora correlates much better with non-invasive, 2D radiographically derived micro-structural and macro-anatomic indices than with BMD. J Bone Miner Res 18(Supp 2):M107

19. Nazarian A, Muller J, Zurakowski D, Muller R, Snyder BD (2007) Densitometric, morphometric and mechanical distributions in the human proximal femur. J Biomech 40:2573–2579
20. Hildebrand T, Laib A, Muller R, Dequeker J, Ruegsegger P (1999) Direct three-dimensional morphometric analysis of human cancellous bone: microstructural data from spine, femur, iliac crest, and calcaneus. J Bone Miner Res 14:1167–1174
21. White SC, Rudolph DJ (1999) Alterations of the trabecular pattern of the jaws in patients with osteoporosis. Oral Surg Oral Med Oral Pathol Oral Radiol Endod 88:628–635
22. Russ JC (1999) The image processing handbook. CRC, Boca Raton
23. Soille P, Rivest J (1996) On the validity of fractal dimension measurements in image analysis. J Vis Commun Image Represent 7:217–229
24. Kleinbaum DG, Kupper LL, Muller KE (1988) Applied regression analysis and other multivariable methods. PWS, Boston
25. Uchiyama T, Tanizawa T, Muramatsu H, Endo N, Takahashi HE, Hara T (1999) Three-dimensional microstructural analysis of human trabecular bone in relation to its mechanical properties. Bone 25:487–491
26. Lespessailles E, Jullien A, Eynard E, Harba R, Jacquet G, Ildefonse JP, Ohley W, Benhamou CL (1998) Biomechanical properties of human os calcanei: relationships with bone density and fractal evaluation of bone microarchitecture. J Biomech 31:817–824
27. Lochmuller EM, Poschl K, Wurstlin L, Matsuura M, Muller R, Link TM, Eckstein F (2008) Does thoracic or lumbar spine bone architecture predict vertebral failure strength more accurately than density? Osteoporos Int 19:537–545
28. Lochmuller EM, Kristin J, Matsuura M, Kuhn V, Hudelmaier M, Link TM, Eckstein F (2008) Measurement of trabecular bone microstructure does not improve prediction of mechanical failure loads at the distal radius compared with bone mass alone. Calcif Tissue Int 83:293–299
29. JT PP, Lochmuller EM, Kuhn V, Nieminen MT, Eckstein F (2008) Experimental hip fracture load can be predicted from plain radiography by combined analysis of trabecular bone structure and bone geometry. Osteoporos Int 19:547–558
30. Parfitt AM (1992) Implications of architecture for the pathogenesis and prevention of vertebral fracture. Bone 13(Suppl 2):S41–47
31. Keaveny TM, Hoffmann PF, Singh M, Palermo L, Bilezikian JP, Greenspan SL, Black DM (2008) Femoral bone strength and its relation to cortical and trabecular changes after treatment with PTH, alendronate, and their combination as assessed by finite element analysis of quantitative CT scans. J Bone Miner Res 23:1974–1982
32. Steines D, Arnaud D, Liew S, Vargas-Voracek R, Bauer DC, Cummings SR, Hess P (2005) Predicting hip fracture in a subgroup of subjects from the study of osteoporotic fracture using automated structural measurement of proximal femur in pelvic radiographs. J Bone Miner Res 20(Suppl 1):S66